Microstrip Discontinuity Capacitances and Inductances for Double Steps, Mitered Bends with Arbitrary Angle, and Asymmetric Right-Angle Bends

PETER ANDERS AND FRITZ ARNDT

Abstract—**The equivalent capacitances and inductances for microstrip double steps, mitered bends with arbitrary angle, and asymmetric right-angle bends are calculated by the moment method. The data for the double step include the coupling effect between the two single steps. The geometry of the mitered bend with arbitrary angle is determined for minimized bend VSWR over a wide range of parameters. The equivalent circuit data of the asymmetric right-angle bend are compared with results of the frequency dependent planar waveguide model.**

I. Introduction

FOR COMPUTER-AIDED design of microwave circuits microstrip discontinuities are often represented by equivalent circuit parameters [1]–[11]. Benedek and Silvester calculated the equivalent capacitance of symmetrical right-angle bends [6] and of steps in the microstrip line [7]. This was also done by Farrar and Adams using a somewhat different approach [8]. Gopinath, Easter, Thomson, and Stephenson [9]–[11] extended the analysis to the equivalent inductance. Recently, equivalent circuit data have been calculated for microstrip bends with arbitrary angle and with curved transition [12]. The calculation of the microstrip bend in [12] has been compared with results of a waveguide model theory [13], [14] which confirms the validity of the quasi-static approach up to about 9 GHz for usual bend geometries.

In this paper the equivalent capacitances and inductances of some other interesting microstrip discontinuities shown in Fig. 1 are calculated by the moment method. The double step (Fig. 1(b)) is often used in microwave circuits as a quasi-lumped inductance or capacitance [1]–[5]. It is shown that a substantial error exists if, as in the past, the coupling effect between the two single steps is neglected. The mitered bend with arbitrary angle (Fig. 1(c)) is of considerable interest for designing matched microstrip circuits. The miter geometry for minimized bend VSWR is determined over a wide range of practical parameters. The results are compared with some available experimental data. The third example, the asymmetrical right-angle bend (Fig. 1(d)), is found for instance in microstrip phase shifter structures, e.g., [16]. It combines the effects of sudden change of width and of a sharp bend.

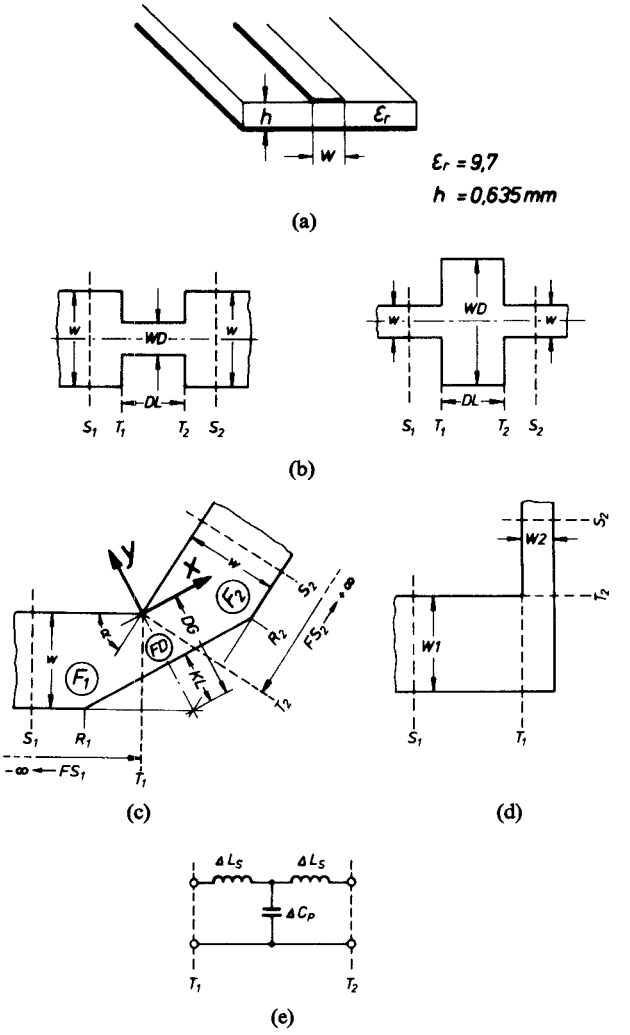

Fig. 1. Investigated microstrip discontinuities. (a) Microstrip line. (b) Double step. (c) Mitered bend with arbitrary angle. (d) Asymmetric right-angle bend. (e) Equivalent circuit for all discontinuities.

Manuscript received March 3, 1979; revised July 10, 1980.

P. Anders was with the Department of Microwaves, University of Bremen, Kufsteiner Str. D-28, Bremen 33, West Germany. He is now with the Deutsche ITT Industries, Hans-Bunte-Str. 19, D-7800 Freiburg, West Germany.

F. Arndt is with the Department of Microwaves, University of Bremen, Kufsteiner Str., D-2800 Bremen 33, West Germany.

0018-9480/80/1100-1213$00.75 ©1980 IEEE

II. Method

The computational methods used are similar to those used before [6]–[12], [20] and thus the theoretical formulation can be abbreviated. As in [9] the reference planes S_1, S_2 (Fig. 1) are chosen so as to include a satisfactorily large proportion of the fringing field of the discontinuity in the region of T_1, T_2.

By plotting the amplitude of the surface current versus the coordinates x and y it was seen that the disturbance by the step is practically negligible beyond a distance approximately equal to the actual line width w_1 or w_2, respectively, (cf. also [7], [21]). Similar results are found for the double step. For the microstrip bend (Fig. 1(c)), however, the fringing field is more intense. It was taken into account within the region $\overline{S_1R_1}=\overline{S_2R_2}\approx 1.5w$, $\approx 3w$, $\approx 6w$ for a 45°, 90°, 120° bend, respectively. For the asymmetric bend (Fig. 1(d)) the corresponding values are $3w_1$, and $3w_2$, respectively.

For determination of the equivalent capacitance ΔC_p the microstrip discontinuity is subdivided into suitable rectangular subsections with the dimensions $\Delta l_n, \Delta b_n$ where the charge density σ is assumed to be constant (pulse expansion). The ground plane is assumed to be at zero potential and the conducting strip to be at a potential of $\Phi = 1$ V. The equivalent capacitance ΔC_p is

$$\Delta C_p = \frac{1}{\Phi} \sum_{m=1}^{M} (\sigma_{um} \cdot \Delta l_m \cdot \Delta b_m) + C_{\text{inf}} \tag{1}$$

with

$$C_{\text{inf}} = \frac{1}{\Phi} \sum_{m=1}^{ND} \sigma_{km} \cdot \Delta l_m \cdot \Delta b_m \tag{2}$$

ND number of the known substrip charge densities σ_k within the region T_1, T_2 due to the infinite strip;

M total number of finite subsections within S_1, S_2;

σ_{km} known value of the mth substrip or subsection charge density due to the infinite strip.

The unknown charge densities σ_{um} are obtained by matrix inversion

$$(\sigma_{um}) = (D_{VF})^{-1}(\Phi_{\text{dif}}) \tag{3}$$

with

$$\Phi_{\text{dif}} = \Phi(P_m) - \left[\sum_{n=1}^{N1} D_{VS}(P_m, P_n')\sigma_{kn}(P_n') + \sum_{n=1}^{ND} D_{VF}(P_m, P_n')\sigma_{kn}(P_n') + \sum_{n=1}^{N2} D_{VS}(P_m, P_n')\sigma_{kn}(P_n') \right] \tag{4}$$

where

$N1, N2$ number of semi-infinite substrips ending at T_1, T_2, respectively;

P_m field point (x_m, y_m, z_m);

P_n' source point (x_n', y_n', z_n'); and

$$D_{VF} = \int_{\Delta x}\int_{\Delta y} G(x, y | x', y')\, dy'\, dx' \tag{5}$$

(source function of the finite subsection with the dimension $\Delta x, \Delta y$)

$$D_{VS} = \int_{\Delta y} \lim_{\Delta x \to \infty} \int_{\Delta x} G(x, y | x', y')\, dx'\, dy' \tag{6}$$

(source function of the semi-infinite substrip ($\Delta x \to \infty$)); where G = Green's function [19].

The equivalent inductances ΔL_S are determined using the current loops method [9]. To include all discontinuity geometries investigated the current loops are not required to be rectangular.

The equivalent inductance is

$$2\Delta L_s = \frac{1}{I_t^2} \int_F \vec{A}\vec{K}\, dF \tag{7}$$

where I_t is the total current flowing into or out of the discontinuity. The vector potential A at the field point P can be separated into the parts

$$A(P) = \int_{FS_1} \boldsymbol{K}_{k1} G_c\, dFS_1 + \int_{FS_2} \boldsymbol{K}_{k2} G_c\, dFS_2 + \int_{F_1} \boldsymbol{K}_{u1} G_c\, dF_1 + \int_{F_2} \boldsymbol{K}_{u2} G_c\, dF_2 + \left(\int_{FD} \boldsymbol{K}_{kD} G_c FD + \int_{FD} \boldsymbol{K}_{uD} G_c\, dF D \right) \tag{8}$$

where

$\boldsymbol{K}_{k1}, \boldsymbol{K}_{k2}, \boldsymbol{K}_{kD}$ known surface currents of the substrips outside of T_1, T_2, and within T_1, T_2, respectively, due to the infinite strip

$$G_c = \frac{\mu_0}{4\pi} \left[\frac{1}{\sqrt{(x-x')^2 + (y-y')^2}} - \frac{1}{\sqrt{(x-x')^2 + (y-y')^2 + 2h^2}} \right] \tag{9}$$

FS_1, FS_2, F_1, F_2, FD = areas (cf., Fig. 1(c)).

The unknown surface currents $\boldsymbol{K}_u$ are obtained by requiring the magnetic induction B_{normal} penetrating into the strip to zero

$$B_{\text{normal}} = 0 = \sum_{i=1}^{N_1} I_{k1i} Q_{BS_{i,j}} + \sum_{i=1}^{N_2} I_{k2i} Q_{BS_{i,j}} + \sum_{i=1}^{ND} I_{kD_i} Q_{BF_{i,j}} + \sum_{i=1}^{M} \sum_{n=1}^{4} I_{ui} Q_{BF_{ijn}} \tag{10}$$

with

N_1, N_2, ND number of the known substrip currents I_k outside of T_1, T_2, and within T_1, T_2, respectively;

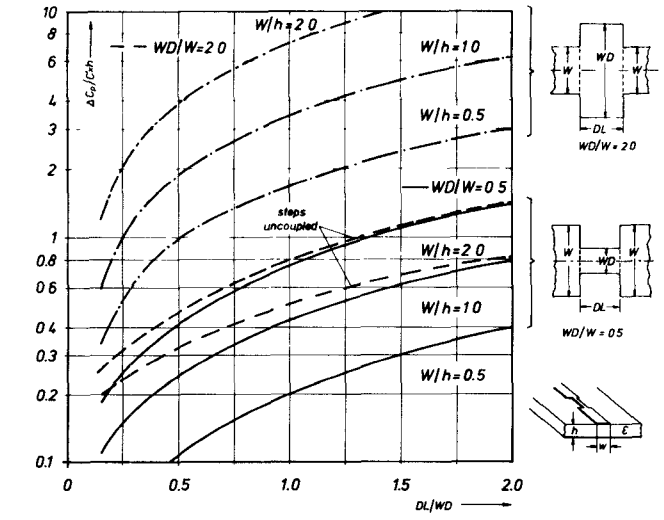

(a)

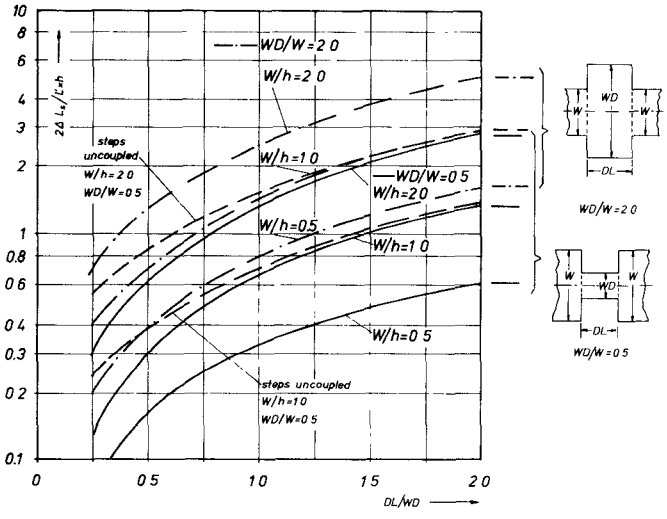

(b)

Fig. 2. Normalized equivalent values of the double step including the coupling effect of the two steps. The dashed lines (---) represent values according to [7], [10], and [11] not including the coupling effect. (a) Equivalent capacitance ΔC_P for $WD/W=2$ (—·—) and $WD/W=0.5$ (——). (b) Equivalent inductance ΔL_S for $WD/W=2$ (—·—) and $WD/W=0.5$ (——). The equivalent values are normalized to the values C', L' of the infinite uniform strip and the height h of the dielectric.

M total number of the unknown loop currents I_u in the four-cornered loop

$$Q_{BF} = -\frac{\partial}{\partial y}\left[\int_{\Delta x} G_c(x, y|x', y')\,dx'\right] \tag{11}$$

$$Q_{BS} = -\frac{\partial}{\partial y}\left[\lim_{\Delta x \to \pm\infty} \int_{\Delta x} G_c(x, y|x', y')\,dx'\right] \tag{12}$$

(source functions). A computer program was developed including (1)–(4), and (7)–(10) for calculating the discontinuity capacitances and inductances.

III. Results

Fig. 2 show the normalized equivalent capacitance ΔC_p and inductances ΔL_S of the entire double step (Fig. 1b) including so the mutual coupling effect of the two steps (solid and dotted lines). The dashed lines represent the values obtained if no coupling effect is considered according to [7], [10], and [11]. It is obvious that, particularly for short relative strip lengths DL/WD, the mutual coupling effect must be taken into account, since the known single step model is based on the assumption of infinitely long uniform strips on both sides and thus leads to wrong results.

In Fig. 3(a)–(c) the normalized equivalent capacitance $\Delta C_p^N = \Delta C_p/(C'\cdot h)$ (dashed line) and inductance $2\Delta L_S^N(L'\cdot h)$ (solid line) of the mitered bend are shown as a function of the miter percentage

$$M = \frac{KL}{DG}\cdot 100 \text{ percent} \tag{13}$$

for various values of the bend angle α and for $\omega/h=0.5$, 1, and 2.

The optimum miter percentage M for minimized bend VSWR can be found approximately if the characteristic impedance Z_W of the equivalent circuit (Fig. 1(e)) is equal to the characteristic impedance Z_0 of the microstrip line which for simplicity is assumed to be quasistatic

$$Z_W = \sqrt{\frac{2\Delta L_S}{\Delta C_p} - \omega^2 \Delta L_S^2} \approx \sqrt{\frac{2\Delta L_S}{\Delta C_p}} = Z_0 \approx \sqrt{\frac{L'}{C'}}\,. \tag{14}$$

This means that the points of intersection for $\Delta C_p^N = 2\Delta L_S^N$ in Fig. 3 approximately indicate the optimum miter percentage.

The optimum miter is shown to be dependent on ω/h (Fig. 4). For the 90° and the 45° bend the results are compared with Douville and James' empirical values [15] which are considered there to be accurate within ±4 percent. The two results agree within about 5 percent if the ±4-percent limit is not taken into account. For the 90° bend of the 50-Ω line the optimum miter percentage given by Kelly *et al.* [17] is also indicated. Our result for the 50-Ω line 90° bend lies between the values given by [15] and [17]. For bend angles of 70° and 110°, $\omega/h=1$ ($h=0.635$ mm), some copper metallized mitered bends have been constructed on Al_2O_3 substrate material ($\epsilon_r \approx 9.7$). To reduce the influence by the coax-to-microstrip transitions to the measurement of the bend VSWR a time domain reflectometer measurement was used to locate the impedance discontinuities within the bend region. For constructed bends with miter percentages of $M_{opt} \approx 50$ percent (70° bend) and $M_{opt} \approx 80$ percent (110° bend) which are indicated in Fig. 4 the maximum VSWR measured within the bend region was <1.005 and <1.01, respectively.

Fig. 5(a), (b) show the normalized equivalent circuit parameters of the unsymmetrical right-angle bend. To compare the quasi-static approach (moment method) used here with the frequency dependent planar waveguide model for the right-angle bend [18] the reflection coefficient $/S_{11}/$ and the transmission coefficient $/S_{21}/$ have been calculated. For low frequencies the two models agree well (cf. Fig. 6(a), (b)). For high frequencies the quasi-static

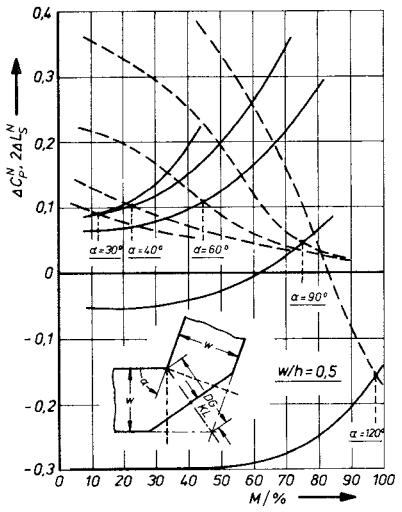

(a)

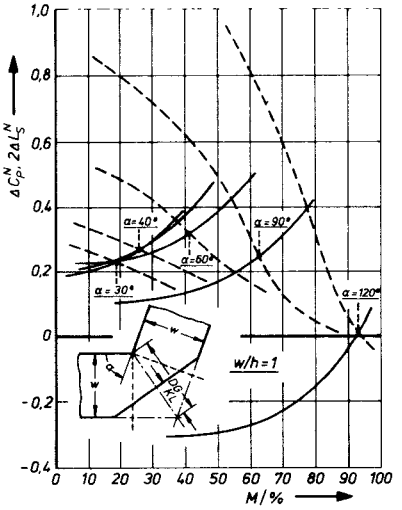

(b)

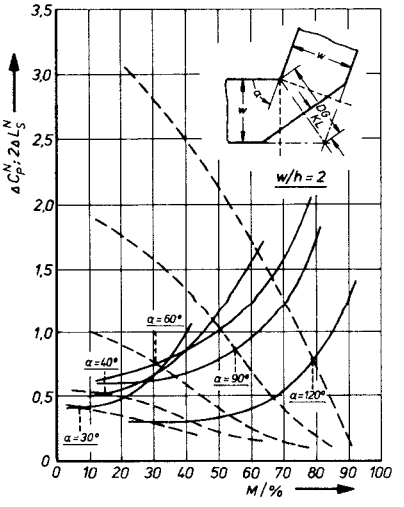

(c)

Fig. 3. Normalized equivalent capacitance $\Delta C_P^N = \Delta C_P/(C' \cdot h)$ (dashed line) and inductance $2\Delta L_S^N/(L' \cdot h)$ (solid line) of the mitered bend as a function of the miter percentage $M = KL/I \cdots 100$ percent. (a) $w/h = 0.5$. (b) $w/h = 1$. (c) $w/h = 2$.

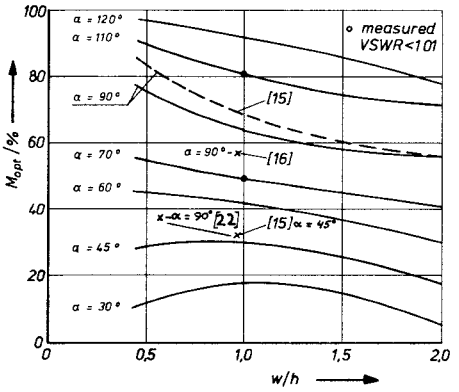

Fig. 4. Optimum miter M_{opt} in percent for minimized bend VSWR of a mitered bend as a function of w/h for bend angles $\alpha = 30° \cdots 120°$.

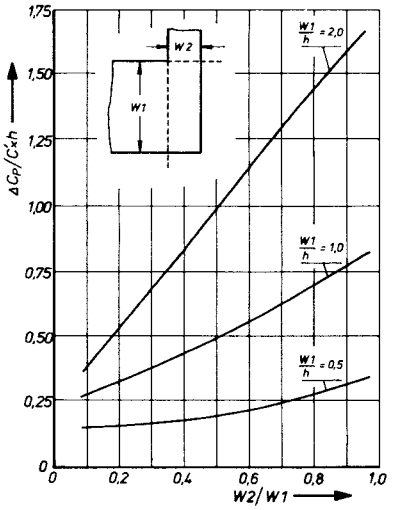

(a)

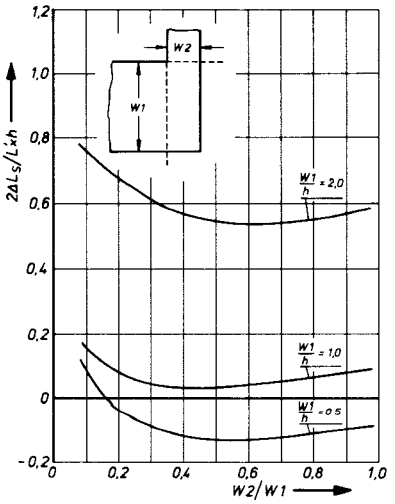

(b)

Fig. 5. Asymmetric right-angle bend. (a) Normalized equivalent capacitance. (b) Normalized equivalent inductance.

approach leads to wrong results because the higher order modes cannot be taken into account.

The number of subsections and current loops was chosen to be about 150 for all computations. The dimension

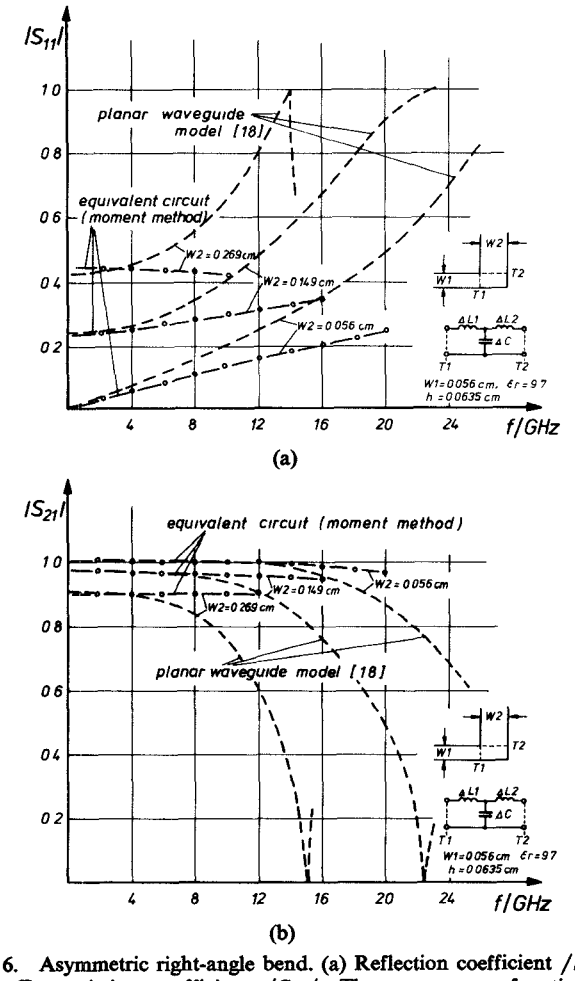

Fig. 6. Asymmetric right-angle bend. (a) Reflection coefficient $/S_{11}/$. (b) Transmission coefficient $/S_{21}/$. These are as a function of frequency, compared with results of a planar waveguide model [18].

of the subsections was varied, with much bigger subsections near that regions where the charge density is nearly uniform. The total computation time for the capacitance data was about 3 min for each data point on the double steps, about 5 min for each mitered bend capacitance computation, and about 10 min for each data point on the asymmetric bend. The corresponding values for the inductances data were about 4 min, 7 min, 15 min, respectively (IRIS 80 computer was used in all computation). The maximum storage required was 120K.

IV. Conclusions

The known matrix methods were applied to often used microstrip discontinuities: double steps, mitered bends with arbitrary angle and the asymmetrical right-angle bend. The equivalent parameters calculated for the double steps include the mutual coupling effect. The data for the mitered bends were used to calculate an optimum miter performance concerning the minimized bend VSWR. These results agree well with experiment and other data reported in the literature [15], [17]. The equivalent circuit data computed for the asymmetric right-angle bend agree very well with results of a planar waveguide model [18] for low frequencies. With reference to [8] it is estimated that the results are accurate to within a few percent.

References

[1] H.-N. Toussaint and R.-K. Hoffmann, "Gegenwärtiger stand und entwicklungstendenzen der rechnergestützten entwicklung von integrierten mikrowellenschaltungen," *Frequenz*, vol. 28, pp. 148–154, 1974.

[2] E. Sanchez-Sinencio and T. N. Trick, "Computer-aided design of microwave integrated circuits," *IEEE Trans. Microwave Theory Tech.*, vol. MTT-22, pp. 309–316, 1974.

[3] J. W. Bandler, P. C. Lin, and H. Tromp, "Integrated approach to microwave design," *IEEE Trans. Microwave Theory Tech.*, vol. MTT-24, pp. 584–591, 1976.

[4] N. M. Hosseini, V. H. Shurmer, and R. A. Soares, "OPTIMAL, a program for optimizing microstrip networks," *Electron. Lett.*, vol. 12, pp. 190–192, 1976.

[5] R. H. Jansen, "Computer-aided design of transistorized microstrip broadband amplifiers on the base of physical circuit structures," *Arch. Elek. Ubertragung.*, vol. AEU-32, pp. 145–152, 1978.

[6] P. Silvester and P. Benedek, "Microstrip discontinuity capacitances for right-angle bends, T-junctions and crossings," *IEEE Trans. Microwave Theory Tech.*, vol. MTT-21, pp. 341–346, 1973.

[7] P. Benedek and P. Silvester, "Equivalent capacitances for microstrip gaps and steps," *IEEE Trans. Microwave Theory Tech.*, vol. MTT-20, pp. 729–733, 1972.

[8] A. Farrar and A. T. Adams, "Matrix-methods for microstrip three-dimensional problems," *IEEE Trans. Microwave Theory Tech.*, vol. MTT-20, pp. 497–504, 1972.

[9] A. Gopinath and B. Easter, "Moment method of calculating discontinuity inductance of microstrip right-angle bends," *IEEE Trans. Microwave Theory Tech.*, vol. MTT-22, pp. 880–883, 1974.

[10] A. F. Thomson and A. Gopinath, "Calculation of microstrip discontinuity inductances," *IEEE Trans. Microwave Theory Tech.*, vol. MTT-23, pp. 648–655, 1975.

[11] A. Gopinath. A. F. Thomson, and I. M. Stephenson, "Equivalent circuit parameters of microstrip step chance in width and cross sections," *IEEE Trans. Microwave Theory Tech.*, vol. MTT-24, pp. 142–144, Mar. 1976.

[12] P. Anders and F. Arndt, "Beliebig abgeknickte mikrostrip-leitungen mit bogenförmigem übergang," *Arch. Elek. Ubertragung.*, vol. AEU-33, pp. 93–99, 1979.

[13] I. Wolff and W. Menzel, "A universal method to calculate the dynamical properties of microstrip discontinuities," in *Proc. 5th European Microwave Conf.*, (Hamburg, Germany), Sept. 1975.

[14] R. Mehran, "Calculation of microstrip bends and Y-junction with arbitrary angle," *IEEE Trans. Microwave Theory Tech.*, vol. MTT-26, pp. 400–405, 1978.

[15] R. J. P. Douville and D. S. James, "Experimental study of symmetric microstrip bends and their compensation," *IEEE Trans. Microwave Theory Tech.*, vol. MTT-26, pp. 175–182, 1978.

[16] Y. Ho Chen, "Microstrip phase shifter provides improved match," *Microwaves*, vol. 18, pp. 44–48, Oct. 1979.

[17] D. Kelly, A. G. Kramer, and F. C. Willwerth, "Microstrip filters and couplers," *IEEE Trans. Microwave Theory Tech.*, vol. MTT-16, pp. 560–562, Aug. 1968.

[18] R. Mehran, "The frequency dependent scattering matrix of microstrip right-angle bends, T-junctions and crossings," *Arch. Elek. Ubertragung.*, vol. AEU-29, pp. 454–460, 1975.

[19] P. Silvester, "TEM-wave properties of microstrip-transmission lines," *Proc. IEEE*, vol. 115, pp. 43–48, 1968.

[20] J. R. Mosig and F. E. Gardiol, "Equivalent inductance and capacitance of a microstrip slot," in *Proc. 7th European Microwave Conf.*, (Copenhagen, Denmark), Sept. 1977.

[21] E. O. Hammerstad and F. Bekkadal, *Microstrip Handbook*, SINTEF Report STF 44, A 74169, Feb. 1975.

[22] V. Biontempo and F. Pucci, Experimental characterization of right-angled bends with varying degree of chamfer," *Alta Freq.*, vol. XLIV, pp. 713–717, Nov. 1975.